2022

Pulmonary Valve Replacement

Mina Shafiei
University of Denver

Pulmonary Valve Replacement

Abstract

Currently, transcatheter pulmonary valve replacement (TPVR) is a well-established alternative for surgical pulmonary valve replacement (SPVR) to treat pulmonary valve disorders in patients with prior congenital heart surgery. Edwards Sapien 3 valve is a bioprosthesis originally designed for the aortic position but has been used off-label in native right ventricular outflow tract (RVOT). It is currently under clinical trial to get food and drug administration (FDA) approval.

This study is a comparison of the performance of Sapien 3 with surgical bioprosthetics. The in vitro tests result showed Sapien 3 experiences less degree of opening and effective orifice area in pulmonic conditions than surgical valves. The less opening area of the leaflets is a concern after TPVR since it may initiate subclinical leaflet thrombosis and valve stenosis over time. Computational results also showed that the maximum in-plane stress value was higher in Sapien 3 than in surgical valves.

Document Type

Thesis

Degree Name

M.S.

Department

Engineering

First Advisor

Ali N. Azadani

Second Advisor

Matt J. Rutherford

Third Advisor

Matt H. Gordon

Keywords

Balloon pulmonary angioplasty (BPA), Food and Drug Administration (FDA), Surgical pulmonary valve replacement (SPVR), Transcatheter pulmonary valve replacement (TPVR)

Subject Categories

Biological Engineering | Biomechanics and Biotransport | Biomedical Engineering and Bioengineering | Engineering

Pulmonary Valve Replacement

_____

A Thesis

Presented to

the Faculty of the Daniel Ritchie School of Engineering and Computer Science

University of Denver

_____

In Partial Fulfillment

of the Requirements for the Degree

Master of Science

_____

by

Mina Shafiei

November 2022

Advisor: Dr. Ali Azadani

Author: Mina Shafiei
Title: Pulmonary Valve Replacement
Advisor: Dr. Ali Azadani
Degree Date: Novemebr 2022

Abstract

Currently, transcatheter pulmonary valve replacement (TPVR) is a well-established alternative for surgical pulmonary valve replacement (SPVR) to treat pulmonary valve disorders in patients with prior congenital heart surgery. Edwards Sapien 3 valve is a bioprosthesis originally designed for the aortic position but has been used off-label in native right ventricular outflow tract (RVOT). It is currently under clinical trial to get food and drug administration (FDA) approval.

This study is a comparison of the performance of Sapien 3 with surgical bioprosthetics. The in vitro tests result showed Sapien 3 experiences less degree of opening and effective orifice area in pulmonic conditions than surgical valves. The less opening area of the leaflets is a concern after TPVR since it may initiate subclinical leaflet thrombosis and valve stenosis over time. Computational results also showed that the maximum in-plane stress value was higher in Sapien 3 than in surgical valves.

Acknowledgments

I would like to express my most profound appreciation to my advisor Dr. Ali Azadani for his invaluable patience and support. I would also like to thank him for his financial support in finishing this Masters program. I believe this thesis would not have been completed without his support and effort.

I am also grateful to my committee members, Dr. Matt Gordon and Dr. Matt Rutherford, who generously advised to improve this thesis. Thanks should also go to my friends and colleague in DU Cardiovascular Biomechanics Lab at the University of Denver who worked with me during this program.

I could not have undertaken this journey without the help, support, and encouragement of my dearest siblings, Nasim and Soroush, and my parents, Narges and Alireza. This thesis is dedicated to them.

Table of Contents

List of Figures

List of Tables

Chapter One: INTRODUCTION

1.1. Anatomy and Physiology of Heart

The heart is responsible for pumping blood to the body. Both pulmonary and systematic circulations are managed by the heart's right and left sides, respectively. Each side of the heart consists of two chambers and two valves shown in Fig. 1.1. The upper chambers, called atrium chambers, receive the blood and the lower chambers, called ventricular chambers, act as pumps to be able to pump the blood. The duty of the valves is to ensure that the blood flow is unidirectional and there is no backflow. Tricuspid and pulmonary valves are on the right, and mitral and aortic valves are on the left side of the heart. The deoxygenated blood enters the right atrium and passes through the tricuspid valve into the right ventricle. Then, it is pumped out to the lungs through the pulmonary valve for the oxygenation process; this process is called the pulmonary circulation. Then, the blood returns to the left atrium and finds its path to the left ventricle using the mitral valve. The left ventricle is the heart's most powerful muscle, which is responsible for pumping blood throughout the whole body using aortic valve and aorta, called systematic circulation (Chandran, Rittgers, and Yoganathan 2006). Each cardiac cycle is divided into two parts – systole and diastole. During systole, the heart muscles contract to provide enough pressure for pulmonary and systematic circulation. On the other hand, during diastole, the heart muscles are relaxed, and atriums receive blood from veins. The duration of systole and diastole are $\frac{1}{3}$ and $\frac{2}{3}$ of a cardiac cycle, respectively.

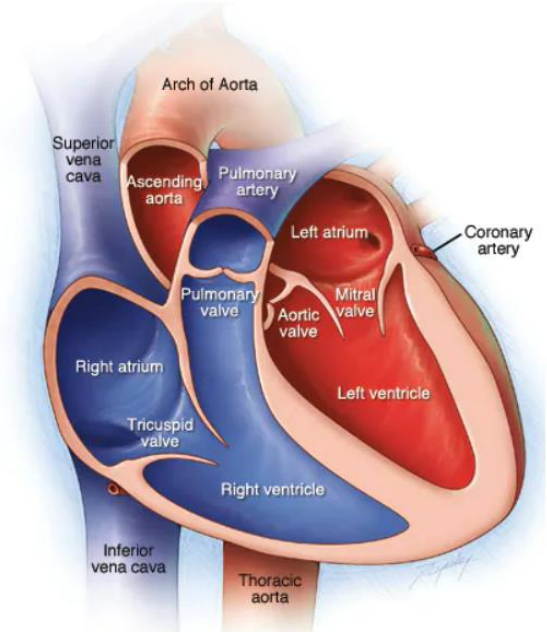

Figure 1.1: Anatomy of heart (courtesy of www.mayoclinic.org)

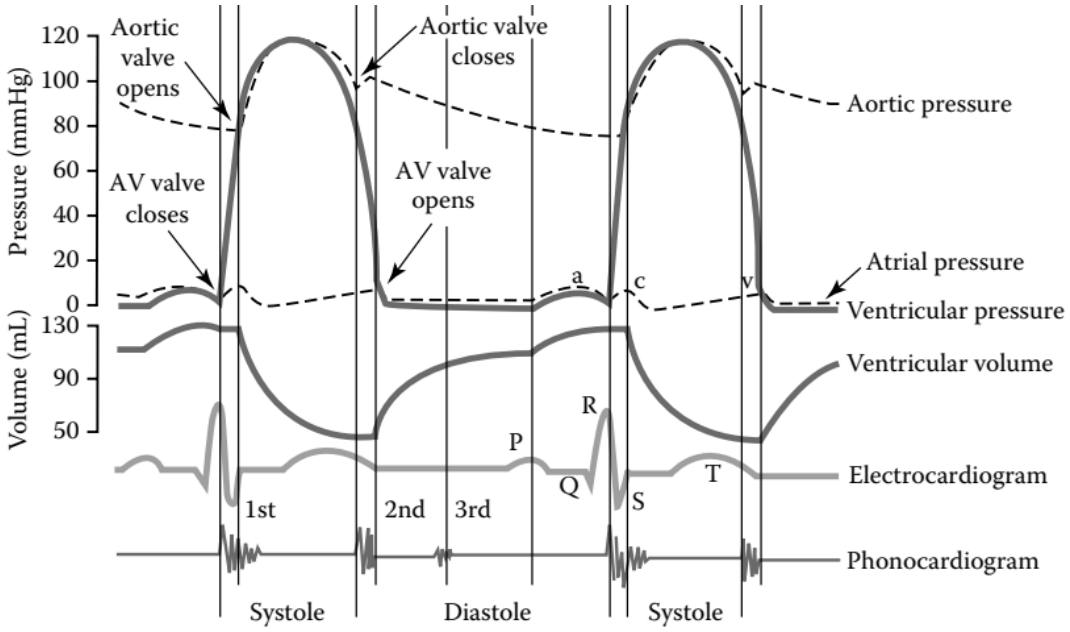

Figure 1.2: Aortic blood pressure waveform for a healthy adult adapted from (Chandran, Rittgers, and Yoganathan 2006)

The aortic pressure in a healthy adult is 80 mmHg at the beginning of systole and goes up to 120 mmHg in the diastole. An aortic pressure waveform for a typical adult is shown in Figure 1.2. However, the maximum ventricular pressure on the pulmonary side is as low as 20 mmHg, while in pediatrics, the maximum aortic and pulmonic pressures are 80 mmHg and 20 mmHg.

1.2. Pulmonary Valve Disease

Heart valve disease is one of the prevalent forms of heart disease and is defined as any kind of disruption in the unidirectional performance of the heart valve. It includes fully opening and closing of the valves during systole and diastole. Two common heart valve disorders are stenosis and regurgitation. Stenosis is primarily a congenital condition in which the valve orifice narrows, and the heart cannot fully open the valve. This may occur by leaflet thickening over time as a result of calcification. On the other hand, regurgitation is incomplete apposition of leaflets leading to backflow. Both primary and secondary causes may result in valve regurgitation.

1.2.1. Congenital Heart Disease

Among four heart valves, the pulmonary valve is the least studied because of its challenging location, which is not accessible by standard echocardiography. Pulmonary valve disorders are primarily congenital. Congenital heart disease includes any birth defect that disrupts the heart's normal function. Tetralogy of Fallot (TOF) is the most common

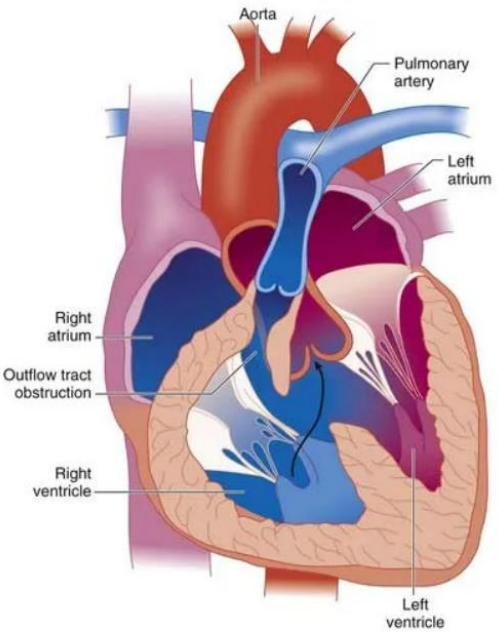

Figure 1.3: Right ventricular outflow tract obstruction and septal defect, both defects are the main features of a congenital disease called Tetralogy of Fallot (courtesy of www.basicmedicalkey.com)

form of congenital heart disease, first introduced by Niels Stenson in 1671. It has four cardinal features: ventricular septal defect, overriding of the aorta, right ventricular outflow tract obstruction, and right ventricular hypertrophy. While the exact cause of TOF is still unknown, about 3-5% of infants are born with it every year.

Among these four forms of TOF, right ventricular outflow tract (RVOT) obstruction is the most prevalent, resulting in severe pulmonary insufficiencies, chronic load, and right ventricular dilation. Intervention is required immediately after birth in the cases of low pulmonary blood flow or cyanosis. In the absence of surgical methods a few decades ago, about 50% of patients with TOF died in the first few years of their life. However, now

almost every patient undergoes a surgical correction after born and survives to their adulthood; this surgical correction must preserve the functionality of the right ventricular and pulmonary valve. These adults usually have no complications in the first 30 years of their life; however, the risk of heart failure, exercise intolerance, and sudden death increases. Therefore, nowadays, more adults with congenital heart disease than before require a new understanding of the complications they face because they need to survive and provide better treatments for children (Apitz, Webb, and Redington 2009).

1.2.2. Ross Procedure

The patients undergoing the Ross procedure are another group of people with RVOT obstruction resulting in pulmonary valve insufficiencies. As a result of Ross procedure for treating aortic valve disorders, the surgeon disrupts the integrity of the pulmonary valve and replaces the aortic valve with pulmonary autograft, another cause of RVOT conduit dysfunction in pediatric patients. Untreated conduit dysfunction results in moderate to severe pulmonary insufficiencies, which itself causes right ventricle dilation (Nordmeyer et al. 2009).

1.3.Pulmonary Valve Replacement

Heart valve replacement is a process in which an artificial valve replaces a patient's biological valve. There are different types of valve replacement, including surgical valve replacement, balloon angioplasty, and transcatheter valve replacement. Surgical valve replacement is an approach in which the surgeon removes the native valve through open-

heart surgery and replaces it with a mechanical or bioprosthetic valve. On the other hand, transcatheter valve replacement and balloon angioplasty are less invasive, percutaneous approaches. We thoroughly discussed the likelihood of valve failure and the need for reoperation for different types of valve replacement in the following sections.

1.3.1. Balloon angioplasty

A treatment option for pulmonary valve stenosis from severe to a moderate degree is Balloon Pulmonary Angioplasty (BPA). Pulmonic stenosis might occur at the valvular, supravalvular, or subvalvular level. BPA is a less invasive method than surgical approaches with more than 90% success rate in treating stenosis, mainly at the valvular level. It was first introduced by Kan et al., but is now utilized by several cardiologists to relieve isolated pulmonary valve stenosis. This technique is recommended for symptomatic patients who suffer from more than 50 mmHg pressure gradient during a cardiac cycle. BPA includes positioning an expandable balloon catheter across the stenotic valve and inflation to increase the mobility of the leaflets (Rao 2007). After the BPA procedure, right ventricular pressure during systole and pressure gradient onto the pulmonary valve drop significantly, improving right ventricular functionality. Two common complications associated with BPA are recurrence of stenosis and progressive regurgitation; however, it rarely results in

Figure 1.4: Bioprosthetic valve made of bovine tissue (on the left) (courtesy of www.edwards.com), mechanical valve (on the right) (courtesy of www.heartvalvesurgery.com)

right ventricle dilation. Long-term outcomes of BPA are still unknown since the data in long-term follow-ups does not exist (Fathallah and Krasuski 2017). The initial target group of BPA was adults; however, due to its promising results, clinicians started to use this technique for children, and studies showed BPA has excellent outcomes in pediatric patients. Furthermore, a critical factor in using BPA is the ratio of balloon diameter to the pulmonary valve annulus which must be between 1.2 and 1.4 in children and 1.2 in adults. The comparison between surgical approaches and BPA shows that although more significant pressure gradient reduction is associated with the surgery, the occurrence rate and degree of regurgitation are lower among the patients who underwent BPA (Rao 2007). BPA technique has not been changed significantly over the past years. Still, due to improvements in medical technics, the balloon delivery system has been developed and reduced the probability of any injury to the patient's vascular system (Tan et al. 2022).

1.3.2. Surgical Pulmonary Valve Replacement

Surgical Pulmonary Valve Replacement (SPVR) is an option to improve pulmonary blood flow and right ventricular performance. SPVR is a good option for patients with moderate or severe pulmonary valve regurgitation, which is an indication of TOF.

Different artificial pulmonary valves are available in the market, which can be divided into two mechanical and bioprosthetic valves shown in Fig. 1.3. Mechanical valves are more durable since they have been made from stronger materials like carbon and titanium.

Figure 1.5: Different artificial heart valves available in the market (from left to right): (a) Medtronic Open Pivot, St Jude Medical Regent, Sorin Group Bicarbon Slimline, Sorin Group Carbonmedics, On-X Life Technologies, (b) Edwards Lifesciences PERIMO (Kheradvar et al. 2015)

However, the patients need life-long anticoagulation therapy because of high shear stresses on the valve, making it prone to blood clot formation.

The other option used for SPVR is bioprosthetic valves. These valves are usually made from the bovine or porcine pericardium. Life-long anticoagulation is not required for patients with bioprosthetic valves; however, because of valve degeneration, they are less durable than mechanical valves, especially in younger patients since they have stronger immune systems (Head, Çelik, and Kappetein 2017). The other failure mode in bioprosthetic heart valves is calcium deposition and resultant valve thickening, which confine the opening of the valve over time (Fathallah and Krasuski 2017).

1.3.3.Transcatheter Pulmonary Valve Replacement

Transcatheter Pulmonary Valve Replacement (TPVR) is an alternative option for valve replacement that emerged in 2000 for patient with prior congenital heart surgery. In this process, a transcatheter valve is delivered into the native pulmonary valve via a catheter through a large artery or vein. The different available transcatheter pulmonary valve in the market and their development process are discussed in the following paragraphs.

In 2000, Bonhoeffer et al. developed a less invasive technique for pulmonary valve implantation. The valve was harvested from a fresh jugular vein and was sutured into a platinum vascular stent. The valve structure was designed to be delivered with a balloon catheter delivery system. In the first phase of the study, this valve was implanted in 7 lambs. In 6 of the lamb, satisfactory hemodynamic results with normal pulmonary pressure

gradient were reported in the first two months after the implantation. Small pulmonary insufficiencies, however, were revealed in one of the lambs in the early evaluation after valve implantation (Bonhoeffer et al. 2000).

In the next phase, eight patients, including seven children (mean age 12.14 ± 2.3 years) and one adult (age 38 years), with severe pulmonary regurgitation and RVOT obstruction, received an 18 mm expandable biological valve. All patients suffered from exercise intolerance because of severe pulmonary regurgitation and stenosis. Angiographic evaluation after valve implantation showed improvement in the hemodynamic performance of the right ventricular in 6 patients. In the short-term follow-up (mean 10.1 months), patients reported improvement in their clinical symptoms, but the reduction in right ventricular size was suspected. Besides, the long-term durability and valve degeneration concerns remained unanswered (Bonhoeffer et al. 2002).

Melody valve (Medtronic Inc, Minneapolis, MN) is one of the FDA-approved widely used bioprosthetic valves designed for pediatric patients suffering from RVOT conduit dysfunction. It has been commercially available since 2010, and its diameter ranges from 16 mm to 29 mm, making it a good candidate for pediatric patients (Tan et al. 2022). Butera et al. analyzed the Melody valve performance and complications in a large group of patients with a median age of 24. All these patients suffered from pulmonary stenosis, pulmonary regurgitation, or both. Favorable outcomes were achieved immediately after implantation. The major complication associated with the Melody valve was reported as stent fracture

when subjected to excessive forces. The pre-stenting procedure was performed to reduce the risk of fracture inside the patients' bodies; however, studies showed there is still incidence of stent fracture in 25% of the patients two years after implantation—this complication results in valve dysfunction, requiring reintervention after diagnosis (Butera et al. 2013).

Sapien XT (Edwards Lifesciences, Irvine, CA) valve is the second generation of the Sapien valve series. It is made of bovine pericardium sutured on a cobalt-chromium stent. Initially designed for the aortic position, it showed promising results under pulmonic conditions and for dysfunctional RVOT conduits. Thus, it received FDA approval in 2012 for pulmonary valve replacement. Sapien XT valve diameter ranges from 26 mm to 29 mm and provides valves for patients with larger conduits. It also includes a stiffer stent, making it less prone to stent fracture compared to the Melody valve (Shahanavaz et al. 2020).

Venus P-valve (Venus Medtech, Shanghai, China) is another new self-expanding bioprosthesis developed in 2017 for native RVOTs with a diameter ranging up to 33 mm. In a clinical study, Morgan et al. showed Venus P-valve has a high implantation success rate of 97%. However, 27% of patients experienced frame fracture during short-term follow-up. The fractures did not affect the integrity and functioning of the valve, and although satisfactory early outcomes, their long-term performance is still under investigation (Morgan et al. 2019).

Sapien 3 is the newest valve design from the Sapien series. Like Sapien XT, it is originally an aortic bioprosthetic but is also widely used in the pulmonary position. However, its FDA approval is still under investigation for TPVR. Several studies assess the performance of the Sapien series valve after TPVR. Shahnavaz et al. studied the clinical result of Sapien XT and Sapien 3 implantation in the pulmonary position. 774 patients were included in this study (Sapien XT was used in 22%, and Sapien 3 was used in 78%). The short-term follow-ups showed good valve functioning. However, there was still a number of valve regurgitation in patients.

Furthermore, there existed some cases of valve thrombosis, which devastated the functionality of the bioprosthetics. In another cohort, among 200 patients who underwent TPVR, 35% received a Sapien valve. After the median follow-up of 1.1 years, the average RVOT pressure was 14 mmHg, with only 1% severe regurgitation and about 66% trivial to no regurgitation (Spigel et al. 2021). Yet, more data is required to evaluate the long-term performance of these valves (Shahanavaz et al. 2020).

A multicenter COMPASSION (Congenital Multicenter Trial of Pulmonary valve Regurgitation Studying Sapien International Transcatheter Heart Valve) trial is currently running for Sapien 3 valve implantation safety and efficacy to treat RVOT obstruction and pulmonary regurgitation. The 3-year outcomes of this trial showed more than 93% freedom from reintervention and a remarkable decrease from 90% pulmonary regurgitation to only

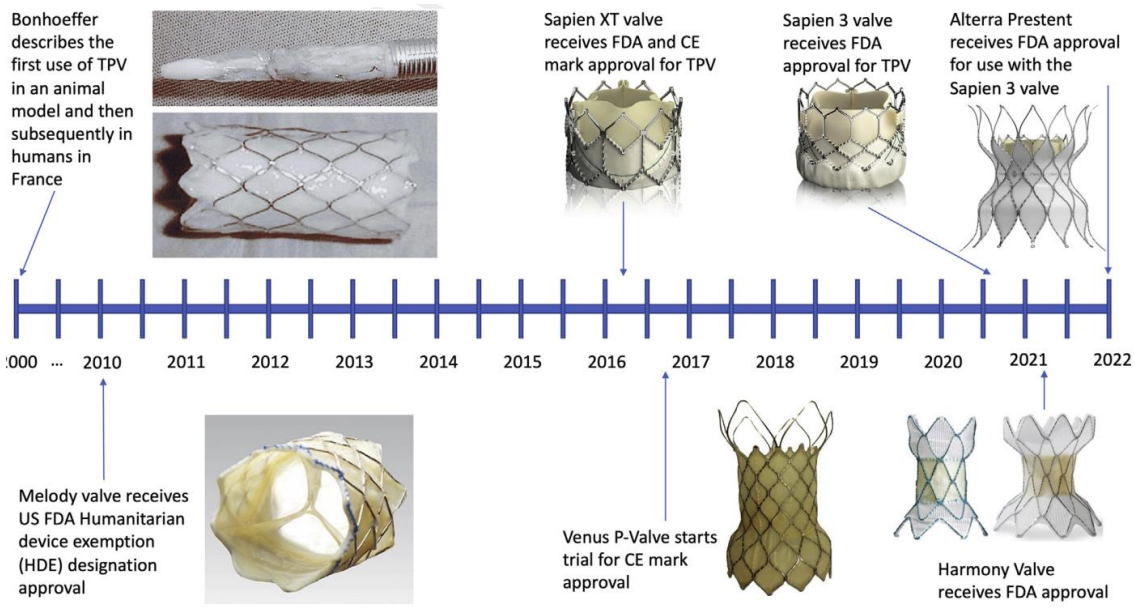

Figure 1.6: Evolution of TPVR over past few decades (Tan et al. 2022)

9% after the implantation. No stent fracture case was recorded during this three years post-implantation (Kenny et al. 2018).

The Harmony (Medtronic, Minneapolis, MN) is a new self-expandable transcatheter pulmonary valve designed for implantation in patients with native RVOTs. It is made of porcine pericardium sutured on a nitinol stent, and in its development pr. Harmony is currently experiencing an early feasibility study phase to get FDA approval and is only available in one size (Bergersen et al. 2017). There is some data regarding favorable 3-year outcomes of implanting Harmony in patients. More than 90% of these patients had no pulmonary regurgitation with no major frame fraction (Benson et al. 2020).

The Alterra adaptive pre-stent (Edwards Lifesciences, Irvine, CA) is a newly developed self-expandable device. Since patients with TOF usually experience RVOT surgical repair or suffer from pulmonary regurgitation, they usually have dilated native RVOTs, requiring larger valve implantation. Alterra modifies these large RVOT morphologies into a proper landing zone for a 29 mm Sapien 3 valve. It is undergoing an early feasibility study to evaluate its clinical performance and get FDA approval. These clinal trials showed encouraging short-term outcomes regarding exercise intolerance improvement and the proper functionality of the pulmonary valve. Still, much more is remained to be done regarding the development of this device (Zahn et al. 2018).

The comparison of SPVR and TPVR shows that length of stay in the hospital is lower in the patients who underwent TPVR. However, there were no significant differences in hospital costs since these patients are projected to have more reintervention rates in the first five years (Daily et al. 2018). On the other hand, the available clinical data show the durability of the bioprostheses is significantly correlated with the patient's age at the time of implantation and the risk of reintervention in children is 5 times greater than in adults. Additionally, studies show the risk of bioprostheses failure rapidly increases after seven years of implantation (Nomoto et al. 2016, Shinkawa et al. 2015, Jang et al. 2012). Therefore, more investigations are required to reassure the privilege of using one treatment option over the other one seems to need more investigations.

1.3.4. Thrombosis

Subclinical leaflet thrombosis was first described in 2013 in a patient following transcatheter aortic valve replacement. It is defined as a hypoattenuating structure in bioprosthetic valve leaflets, which increases the thickness and confines the movement of leaflets. In other words, it includes the growth of a thin layer of thrombus on leaflets. Subclinical leaflet thrombosis is also known as hypo-attenuated leaflet thickening (HALT). This phenomenon is more prevalent after transcatheter valve replacement, and the number of cases of HALT after surgical valve replacement is seemed to be much lower. Patients with subclinical leaflet thrombosis remain asymptomatic; however, it might progress and increase the risks for further events such as embolism and raise concerns regarding the reduction of the long-term durability of the bioprosthetic valves (Rosseel, De Backer, and Søndergaard 2019).

Chapter Two: PULMONARY VALVE REPLACEMENT RISKS AND COMPLICATIONS IN PEDIATRIC PATIENTS

As mentioned before, one of the crucial indications for TOF is RVOT obstruction and pulmonary valve dysfunction. Among currently available valves, the most popular is the Melody valve. Melody transcatheter valve implantation is an option to treat moderate or severe pulmonary regurgitation to non or mild regurgitation up to 5 years after implantation. The risk of reintervention has been reported at about 76% in the same follow-up period. Although the Melody has shown promising clinical performance among the majority of the patients, the risk of reintervention increases significantly among these patients after five years, and the small conduit area of the Melody is no longer able to pump out the required blood volume (Balzer 2019).

Another popular valve for pulmonary valve replacement is the off-label use of aortic bioprosthetics that show the promising result on the left side of the heart. Sapien 3 transcatheter aortic valve is one of the candidates for TPVR. The performance of the Sapien 3 valve in the patients with TOF showed comparable results with the Melody valve under pulmonic conditions in different studies.

Furthermore, limitations in size and proneness to stent fracture associated with these valves increase the tendency towards off-label use of aortic bioprostheses, which have shown promising results on the left side of the heart. On the other hand, the available

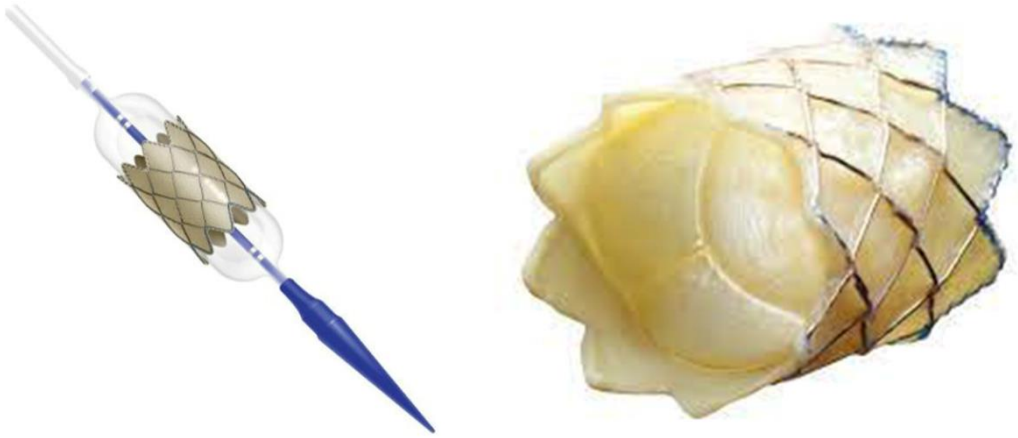

Figure 2.1: Melody valve (right), Melody delivery catheter (left) (courtesy of www.medtronic.com)

clinical data show the durability of the bioprostheses is significantly correlated with the patient's age at the time of implantation and the risk of reintervention in children is 5 times greater than in adults. Studies, additionally, show the risk of bioprostheses failure are rapidly increased after seven years of implantation (Nomoto et al. 2016, Shinkawa et al. 2015, Jang et al. 2012). Therefore, more investigations are required to reassure the long-term outcomes of using aortic bioprostheses under the pulmonic condition in pediatric patients.

Some in-vitro tests have been done to assess the hemodynamic performance of the bioprosthetic valves under pulmonary pressure in adults. However, valve performance and durability are the main concerns in pediatric patients since progressive bioprostheses dysfunction may lead to hemodynamic obstructions. (Shinkawa et al. 2015, Pragt et al. 2020, Ghawi, Kenny, and Hijazi 2012) One of the primary outcomes of pulmonary valve

replacement is treated moderate or severe pulmonary regurgitation. However, there are still some debates about the evolving significant pulmonary regurgitation in long-term follow-ups. Another destructive mechanism after pulmonary valve replacement, called subclinical leaflet thrombosis, associates with reduced leaflet motion at the base of leaflets, where they are less mobile. Studies show larger and under-expanded prostheses during valve valve procedure have a critical role in HALT after transcatheter valve replacement. Several cases were reported with thrombosis after TPVR.(Shahanavaz et al. 2020, DeZorzi et al. 2021, Schneider, Delaney, and Cabalka 2016) According to the limitation of the available studies regarding the short-term follow-up after TPVR, there is still a necessity for closely monitoring the longevity of bioprosthetic valves inside patients' bodies (Spigel et al. 2021).

The present study compared the hemodynamics performance of commercially available transcatheter aortic Sapien 3 with different sizes of surgical aortic Magna Ease and Theon prostheses (Edwards Lifesciences, Irvine, CA), using hydrodynamic tests and computational methods. It also provides a characterization process to find the stress distribution over the leaflets and compare the longevity and probable lifespan of bioprosthetic transcatheter valves to surgical ones. A comparison of the long-term durability of bioprostheses in aortic position using computational techniques is reported in former studies. Higher mechanical stress is observed on transcatheter valves implanted on the left side of the heart comparing to surgical valves, which ultimately may contribute to the long-term durability of the valves. (Abbasi et al. 2019)

2.1.Material and Methods

Two different experimental and computational methods have been used in this study. In the first step, an in-vitro test was performed to assess the hemodynamic performance of bioprosthetic valves in different testing conditions. In the next phase, the structural characteristics of the valves were evaluated by computer finite element simulations. These two steps are described in the following sections in detail.

2.2.1.Valves

19mm, 21mm, 23mm Theon, 25mm Magna Ease surgical valves, and 26mm Sapien3 transcatheter valve (Edwards Lifesciences, Irvine, CA) were used in pulse duplicator testing setup and for further FE simulations and optimizations framework.

2.2.2. Test conditions and setup

A custom-built pulse duplicator setup (BDC Labs, Wheat Ridge, CO, USA) was used for in-vitro testing of the bioprosthetic valves. The heart rate and cardiac output parameters were controlled by the pump using a LabVIEW software. Each pump's stroke changes the pressure around the silicon ventricle and makes the pulsatile flow. Two 3D-printed silicon washers are used to mount the valves onto the silicon heart. The swing ring of the surgical bioprosthetic valves was sutured on top of the washer to be kept in place during the tests. For transcatheter bioprosthetics, a balloon delivery system is used to fully expand the transcatheter valve into the washer at the same level as the bottom of the washer. A bileaflet mechanical valve was installed on the other side of the silicon ventricle. Two compliance

chambers are used downstream of the pulmonary valve to simulate the peripheral resistance of the arteries. The pressure in the pulmonary artery and right ventricle were measured by embedded pressure transducers inside the pulse duplicator setup. These pressure transducers were calibrated before each testing condition using a pressure transducer sensor. An electromagnetic flowmeter also measured the flow (Barakat, Dvir, and Azadani 2018).

Three different test conditions were applied to an in-vitro test summarized in Table 2.1. The conditions for heart rate, cardiac output, and mean pressure gradient of pulsatile flow test, recorded in Table-1, were matched international ISO-5840 for pediatrics and adults on the right and left side of the heart. The same pump profile was used for each test condition. The systolic duration was kept at 35%.

The fluid in the system was 37% by volume Glycerin (99% The Science Company, Denver, CO, USA) and phosphate buffered normal saline solution (Research Products International, Mount Prospect, IL, USA) at 23 °C with the calculated density of 1086.35 $\frac{kg}{m^3}$(Association 1963). From the top view, the leaflet motions were captured using a SONY DSC-RX10M3 at the rate of 960 and 480 frames per second for further hemodynamic analysis. Sapien3 was fully expanded by a balloon in a 3D-printed costume washer.

Table 2.1: Test conditions

Condition	Heart rate (beats/min)	Cardiac Output (L/min)	Mean Pressure Gradient (mmHg)
Adult Aortic	70	5	100
Child Pulmonary Normal Flow	80	3.5	20
Child Pulmonary Low Flow	60	2	20

The postprocessing of the experimental data was completed in Matlab (version R2021a). A low pass filter, with the order of 400 and 250 for surgical valves and Sapien3, respectively, and the cutoff frequency of 4, were applied to the collected pressure gradient data. The value for pressure gradients was later used for finite element analysis of the valves. Different parameters were evaluated by the developed Matlab code. These parameters are:

- Mean Positive Pressure Difference (PPD): Mean PPD is the outflow pressure subtracted from inflow pressure over the period from the start of the forward flow to the end of the outflow to the period in which the outflow pressure is more than the inflow pressure.

$$PPD\ Mean = \frac{\int_{t_{FFStart}}^{t_{PPD}} (P_{inflow}(t) - P_{outflow}(t))dt}{t_{PPD} - t_{FFStart}} \qquad (2.1)$$

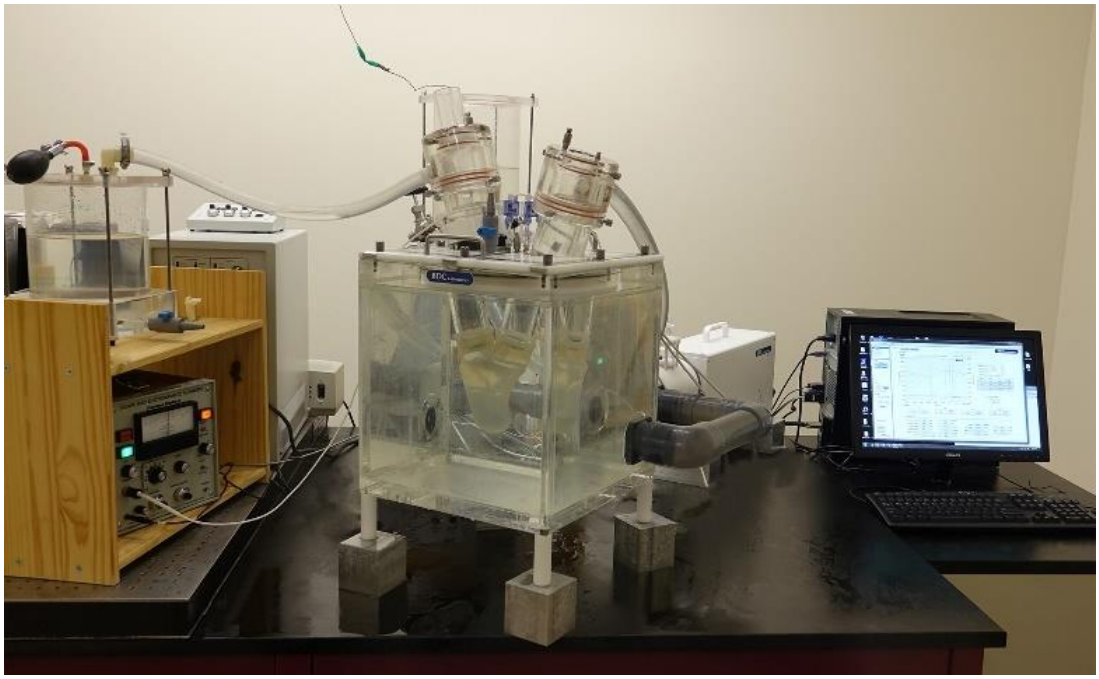

Figure 2.2: Pulse duplicator setup

- Closing Volume: The volume of the flow passing through the valve during the valve closure.
- Closed Volume: The volume of the flow passing through the valve while the valve is closed.
- Total Regurgitant Volume: Total regurgitant flow through the valve is defined as the closing volume plus the closed volume.
- RMS Flow: Root mean square of flow over the period ranging from the forward flow start to the forward flow end.

$$RMS\ Flow = \sqrt{\frac{\int_{t_{FFStart}}^{t_{PPD}} [Flow(t)]^2 dt}{t_{PPD} - t_{FFStart}}} \qquad (2.2)$$

- Effective Orifice Area (EOA): EOS is a metric to evaluate the valve's performance. According to the international ISO 5840, the following equation is used for effective orifice area (EOA) calculation:

$$EOA = \frac{RMS\ Flow}{51.6\sqrt{\frac{PPD\ Mean}{\rho}}} \qquad (2.3)$$

Where RMS Flow is the root mean square of the flow (in ml/s) from the start to the end of the forward flow, PPD Mean is the positive pressure difference (in mmHg), and ρ is the density of the circulatory fluid (in g/cm^3).

2.2.3. 3D modeling of the valves

The valves are scanned by a NextEngine 3D scanner (NextEngine, Inc., Santa Monica, CA). Surface construction was done using Geomagic Design X (version 2020.0.3) and SOLIDWORKS (version 2020). The surface of one leaflet was created with a uniform thickness and used for creating the other leaflets based on symmetry.

The thickness was the mean thickness of three leaflets measured using scanned data and a caliper for each valve. The geometries later were used in Hypermesh (Altair Engineering, Inc., Troy, MI) to generate mesh for further FE analysis. A flexible frame was

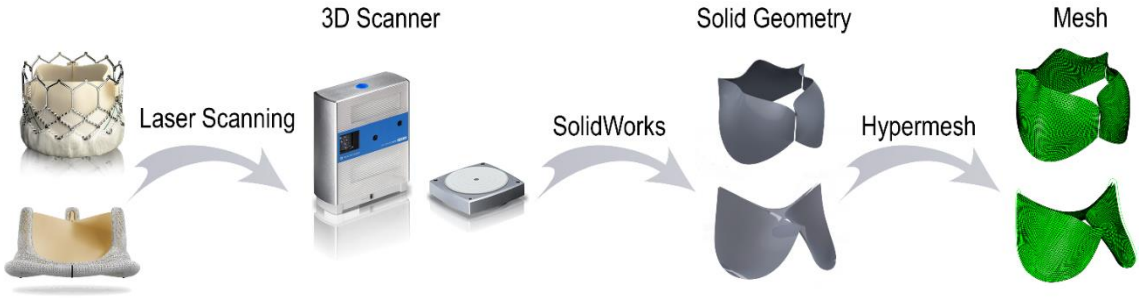

Figure 2.3: Overview of making 3D geometry of the valves

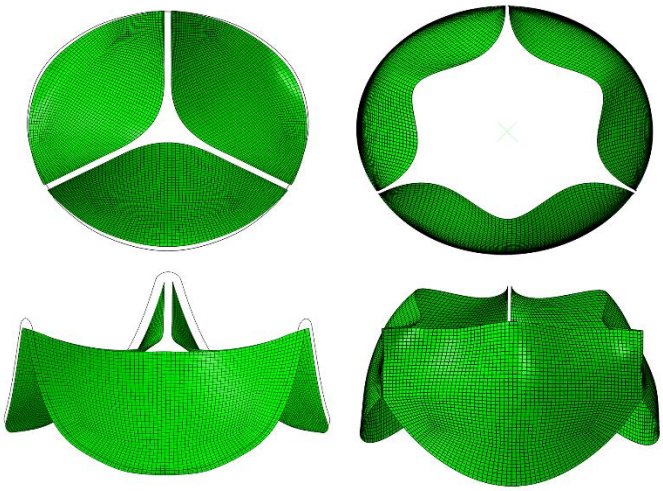

Figure 2.4: Meshed Geometries Sapien 3 (right) and Magna Ease (left)

also developed for a 25 mm Magna Ease valve with a density of 8900 kg/m^3, the Young modulus of 18 GPa, and the Poisson ratio of 0.226.

2.2.4. Optimization framework

For finite element simulations, the material properties of the leaflets are required. These material properties have been found through an optimization process using

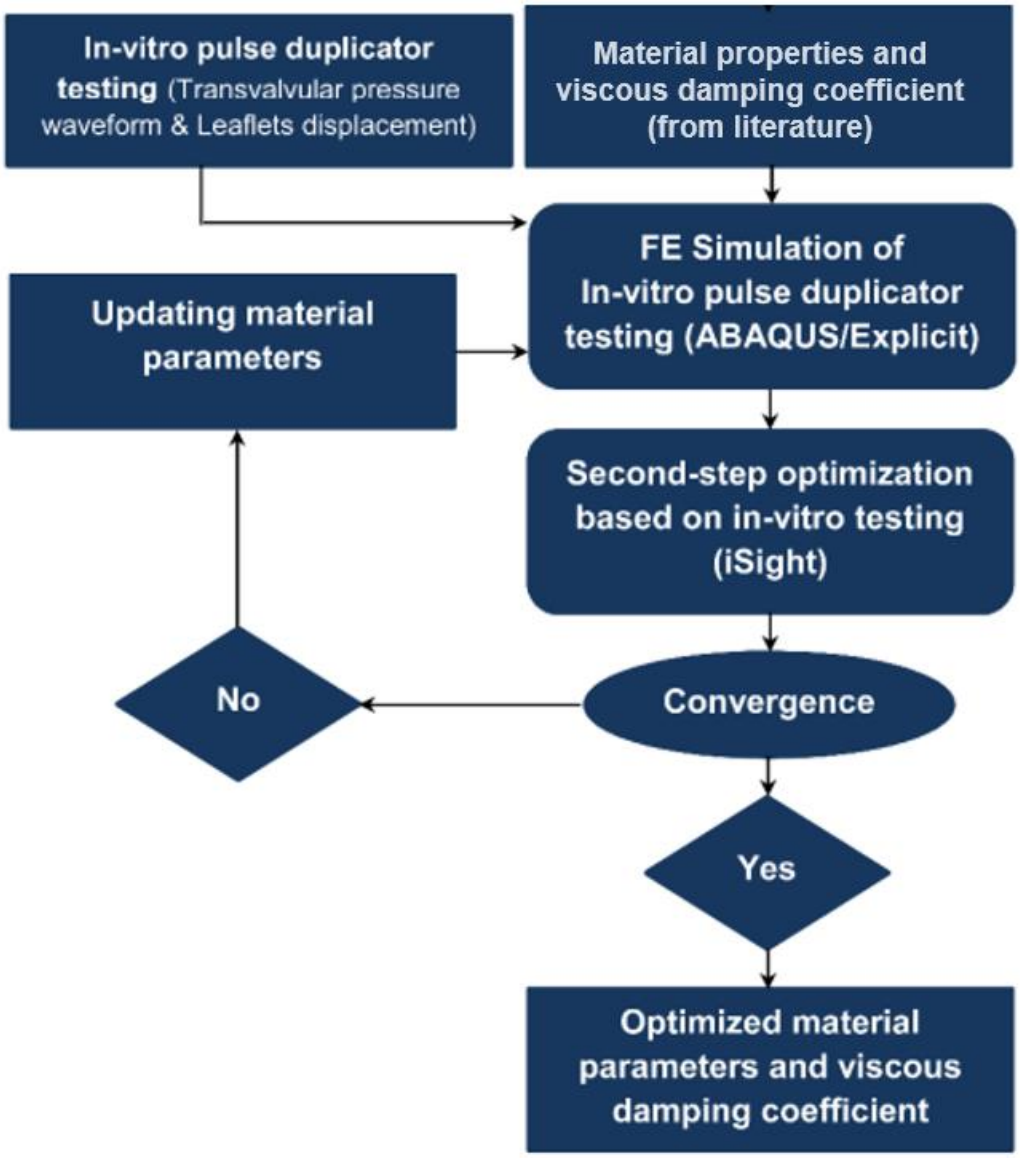

Figure 2.3: Flowchart of material optimization

the result of in-vitro tests. The details about the optimization are discussed in the following paragraphs.

Anisotropic Fung model with a damping coefficient (α), which represents the effect of fluid along the leaflets, was used for the FE simulations to find out of plane material coefficients. Based on the Fung model, the generalized form of strain energy will be:

$$\Psi = \frac{c}{2}(e^{Q} - 1) + \frac{1}{D}(\frac{J_{el}^{2}-1}{2} - \ln J_{el}) \quad (2.1)$$

$$Q = E : (\mathbb{b}E) \quad (2.2)$$

$$\mathbb{b} = \begin{bmatrix} b_{1111} & b_{1122} & b_{1133} & b_{1123} & b_{1113} & b_{1112} \\ & b_{2222} & b_{2233} & b_{2223} & b_{2213} & b_{2212} \\ & & b_{3333} & b_{3323} & b_{3313} & b_{3312} \\ & & & b_{2323} & b_{1323} & b_{1223} \\ & Symmetric & & & b_{1313} & b_{1213} \\ & & & & & b_{1212} \end{bmatrix} \quad (2.3)$$

Where J_{el} is the elastic volume ratio and equals one according to incompressibility assumption, and c and D are temperature-related parameters. $\mathbb{b}$ is a fourth-order symmetric tensor with 21 constants, and E is the Green strain tensor. Material orientations were assigned to the leaflet shell elements with a previously developed MATLAB code by Abbasi et al. (Abbasi et al. 2019). The pressure gradient measured in the pulse duplicator setup was applied to the leaflets. The density of 1100 kg/m^3 was considered for the leaflets. The optimized 21 constants of the Fung model reported in Abbasi et al(Abbasi et al. 2019) for 25 mm Magna Ease and 26 mm Sapien3, used for the optimization framework in Isight, are shown in equations (2.4) and (2.5). The optimization was performed by

minimizing the error between the measured distance of the middle point at the free edge of one leaflet from the center of the valve in 960 fps video frames captured during the pulsatile

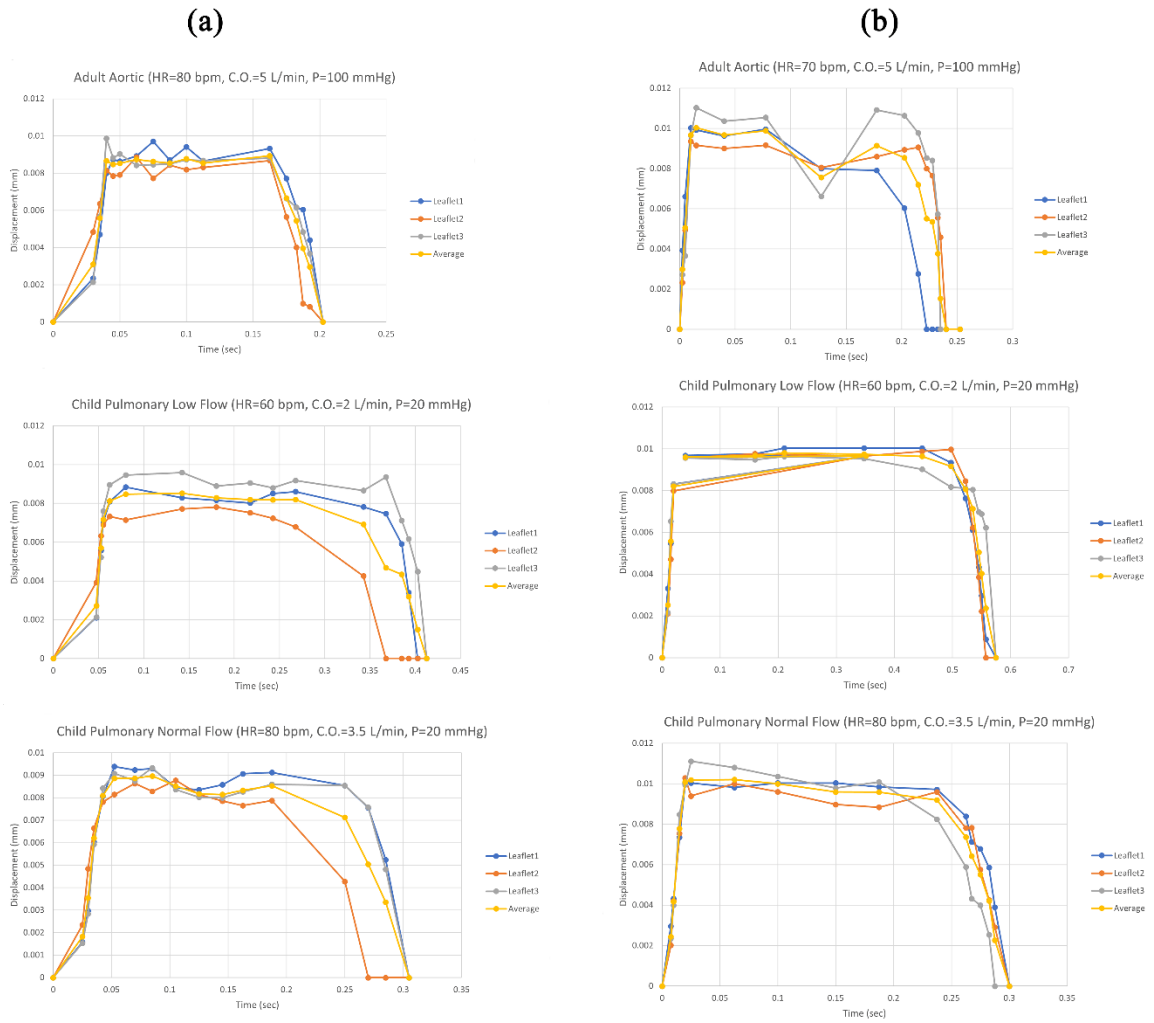

Figure 2.4: Displacement of the middle point of the leaflets in 3 different testing conditions for (a) Magna Ease and (b) Sapien 3 valves; the average of the displacement for each condition has been used for material optimization

test, shown in Figure 2.6, and FE simulations. The result of optimizing c and α coefficients for aortic and pulmonary conditions are presented in Table 2.2.

$$\mathbb{b}_{MagnaEase} = \begin{bmatrix} 63.42 & 31.84 & 51.29 & 17.37 & 49.02 & 39.39 \\ & 63.74 & 46.75 & 68.38 & 63.09 & 19.22 \\ & & 62.82 & 38.51 & 60.17 & 55.50 \\ & & & 14.30 & 15.47 & 28.04 \\ & Symmetric & & & 47.30 & 13.69 \\ & & & & & 67.53 \end{bmatrix} \quad (2.4)$$

$$\mathbb{b}_{Sapien\ 3} = \begin{bmatrix} 87.45 & 37.88 & 56.25 & 18.49 & 45.47 & 37.23 \\ & 83.97 & 43.50 & 70.21 & 71.65 & 25.72 \\ & & 89.93 & 43.70 & 62.41 & 58.98 \\ & & & 13.92 & 15.12 & 27.96 \\ & Symmetric & & & 43.54 & 16.47 \\ & & & & & 68.56 \end{bmatrix} \quad (2.5)$$

Table 2.2: Material parameter and viscous damping coefficient for 3D anisotropic Fung model

Bioprosthesis	Condition	c (material parameter, KPa)	α (viscous damping, 1/s)
Primount Magna Ease	Aortic	90.72	10,642
	Pulmonary	18	2,641
Sapien 3	Aortic	7.8	4,800
	Pulmonary	7.8	1,500

Chapter Three: RESULTS AND DISCUSSION

3.1. Experimental Result

3.1.1. Transvalvular mean pressure gradient

The comparison of mean gradient pressure on the valves shows the overall pressure gradient on the valves was decreased with decreasing the pressure conditions in pulmonary conditions. Besides, as expected, increasing the size of the valves results in less pressure gradient on the valve except for 26 mm Sapien 3 in child pulmonary with low flow. Under reference adult aortic and child pulmonary conditions with normal flow, the pressure difference on the 26 mm Sapien 3 valve (14.66 ± 0.12 mmHg and 8.36 ± 0.05 mmHg, respectively) was lower than the surgical valves. However, in child pulmonary with low flow condition, the pressure gradient on 26 mm Sapien 3 was significantly more than 25 mm Magna Ease ($p < 0.05$). The pressure gradient on the leaflets in child pulmonary condition with the low flow was less than normal flow for all valves.

3.1.2. Effective orifice area

The overall trend of effective orifice area indicates that each valve opened more in adult aortic condition than in child pulmonary because less pressure was applied on the leaflets. Comparing the amount of effective orifice area of surgical valves with 26 mm Sapien 3 valve shows that Sapien 3 significantly experienced more opening than the others in both aortic (1.85 ± 0.03 cm^2, $p < 0.05$) and child pulmonary with normal flow conditions (1.31 ± 0.01 cm^2, $p < 0.05$). However, in a child pulmonary condition with

low flow, the effective orifice area of Sapien 3 was smaller than all sizes of surgical valves except the 19 mm one.

Table 5.1: Mean transvalvular pressure under different testing conditions for each surgical valve size and 26 mm Sapien 3

	Transvalvular Pressure Gradient (mmHg)		
	Adult Aortic Mean ± S.D.	Child Pulmonary Normal Flow Mean ± S.D.	Child Pulmonary Low Flow Mean ± S.D.
19 mm	34.50 ± 0.21	12 ± 0.06	7.30 ± 0.02
21 mm	26.20 ± 0.20	11.67 ± 0.11	7.38 ± 0.02
23 mm	23.6 ± 0.33	10.70 ± 0.02	6.54 ± 0.02
25 mm	17.02 ± 0.14	9.86 ± 0.05	5.04 ± 0.02
26 mm	14.66 ± 0.12	8.36 ± 0.05	6.66 ± 0.03

Table 5.2: Mean effective orifice area under different testing conditions for each surgical valve size and 26 mm Sapien 3

	Effective Orifice Area (cm^2)		
	Adult Aortic Mean ± S.D.	Child Pulmonary Normal Flow Mean ± S.D.	Child Pulmonary Low Flow Mean ± S.D.
19 mm	1.15 ± 0.02	0.76 ± 0.08	0.54 ± 0.02
21 mm	1.41 ± 0.03	0.84 ± 0.01	0.65 ± 0.07
23 mm	1.56 ± 0.02	0.99 ± 0.02	0.61 ± 0.01
25 mm	1.33 ± 0.09	1.08 ± 0.14	0.86 ± 0.07
26 mm	1.85 ± 0.03	1.31 ± 0.01	0.56 ± 0.01

3.1.3. Maximum Opening Area

The maximum opening areas in Sapien 3 valve were more than 25 mm surgical valve in all testing conditions. A decreasing trend was recorded for both 25 mm Magna Ease and 26 mm Sapien 3 in adult aortic, child pulmonary with normal flow, and child pulmonary with low flow conditions. The less opening area on the valves in pulmonary conditions with respect to reference aortic condition may alter the kinematics of leaflets and increase the risk of blood stasis on the transcatheter Sapien 3 valve.

3.1.4. Regurgitation fraction

Reducing the pressure gradient on the valves caused less regurgitant volume in pulmonary conditions than in reference adult aortic. A trend in increasing the volume of regurgitant volume was noticeable in 19 mm (6.77 ± 2.29 ml), 21 mm (9.89 ± 2.26 ml), and 23 mm (14.01 ± 1.93 ml) surgical valves as the size of the valve was increased, but not in 25 mm valve under adult aortic condition. The amount of backflow in a child pulmonary condition with the low flow was less than the corresponding value in normal flow conditions for all surgical valves. The regurgitant volume in 26 mm Sapien 3 in both child pulmonary conditions was more than 25 mm Magna Ease, but it was not statistically significant ($p > 0.05$). The Sapien 3 regurgitations in pulmonary conditions demonstrated paravalvular leakage between the valve and the heart tissue. This amount of backflow in child pulmonary with the low flow was more than regurgitation volumes in all surgical valves.

Table 5.3: Mean maximum opening area under different testing conditions for 25 mm Perimount Magna Ease and 26 mm Sapien 3

	Maximum Opening Area (cm^2)		
	Adult Aortic Mean ± S.D.	Child Pulmonary Normal Flow Mean ± S.D.	Child Pulmonary Low Flow Mean ± S.D.
25 mm	2.92 ± 0.08	2.72 ± 0.09	2.32 ± 0.15
26 mm	3.79 ± 0.10	3.27 ± 0.09	2.53 ± 0.07

Table 5.4: Mean regurgitation volume under different testing conditions for each surgical valve size and 26 mm Sapien 3

	Regurgitation Volume (ml)		
	Adult Aortic Mean ± S.D.	Child Pulmonary Normal Flow Mean ± S.D.	Child Pulmonary Low Flow Mean ± S.D.
19 mm	6.77 ± 2.29	1.50 ± 1.87	1.49 ± 0.87
21 mm	9.89 ± 2.26	7.19 ± 2.89	2.29 ± 1.80
23 mm	14.01 ± 1.93	4.77 ± 1.42	2.85 ± 0.31
25 mm	4.79 ± 2.02	1.19 ± 0.58	1.02 ± 1.01
26 mm	7.59 ± 3.49	4.10 ± 0.91	5.04 ± 1.44

3.1.5. Full closure

The position of the leaflets at the peak of diastole extracted from high-speed videos is shown in Figure 1. Sapien 3 valve reaches full closure in all conditions; however, 21 mm, 23 mm, and 25 mm surgical valves experience some intravalvular leakage in pulmonary conditions. The 19 mm Perimount Theon reaches full closure in both adult aortic and child pulmonary with normal flow but not low flow. This is because less pressure is applied to the valves in pulmonary conditions (20 mmHg) than in aortic reference condition (100 mmHg). The closures of valves under normal (3.5 L/min) were close to complete closure than low cardiac outputs (2 L/min) for 21 mm, 23 mm, and 25 mm surgical valves.

3.1.6. Energy loss

As expected, energy loss in the forward flow is decreasing as the internal diameter of the surgical valves increases; therefore, the 25 mm Magna Ease valve had less energy loss (0.10 ± 0.00 mJ) than the 23 mm (0.32 ± 0.00 mJ), 21 mm (0.26 ± 0.00 mJ), and 19 mm (0.45 ± 0.01 mJ). In addition, by reducing the pressure difference on the valves in pulmonary conditions, the forward flow energy loss is also decreasing compared to adult aortic. In the child pulmonary condition normal flow, the computed energy loss for the forward flow is more than the child pulmonary low flow condition. The same result for closing and leakage energy loss in pulmonary conditions has been recorded.

Table 5.5: Mean energy loss under adult aortic condition for each surgical valve size and 26 mm Sapien 3

	Adult Aortic Energy Loss (mJ) Mean ± S.D.			
	Forward Flow	Closing Flow	Leakage Flow	Total
19 mm	445.40 ± 6.18	2.12 ± 0.55	70.76 ± 20.84	518 ± 21.98
21 mm	262.82 ± 1.76	14.69 ± 1.55	102.06 ± 15.35	387.28 ± 28.42
23 mm	320.54 ± 3.67	4.12 ± 0.91	148.12 ± 20.78	472.79 ± 20.23
25 mm	95.80 ± 1.31	2.24 ± 0.14	39.21 ± 12.92	136.16 ± 13.15
26 mm	136.83 ± 1.60	7.31 ± 1.01	54.87 ± 21.87	198.99 ± 20.67

Table 5.6: Mean energy loss under child pulmonary with normal flow condition for each surgical valve size and 26 mm Sapien 3

	Child Pulmonary Normal Flow Energy Loss (mJ) Mean ± S.D.			
	Forward Flow	Closing Flow	Leakage Flow	Total
19 mm	92.35 ± 0.90	0.5 ± 0.22	2.58 ± 2.42	95.43 ± 2.93
21 mm	75.34 ± 1.72	5.28 ± 0.97	115.90 ± 11.19	196.52 ± 11.75
23 mm	85.87 ± 1.25	1.44 ± 0.35	6.71 ± 2.09	94.31 ± 2.74
25 mm	75.66 ± 0.81	0.73 ± 0.14	2.26 ± 0.56	78.79 ± 1.06
26 mm	63.54 ± 0.68	0.78 ± 0.07	3.25 ± 0.93	67.56 ± 1.06

Table 5.7: Mean energy loss under child pulmonary with low flow condition for each surgical valve size and 26 mm Sapien 3

	Child Pulmonary Low Flow Energy Loss (mJ) Mean ± S.D.			
	Forward Flow	Closing Flow	Leakage Flow	Total
19 mm	46.94 ± 1.24	0.07 ± 0.03	1.47 ± 0.58	48.48 ± 1.62
21 mm	49.00 ± 0.54	0.17 ± 0.06	2.04 ± 1.02	51.20 ± 0.67
23 mm	40.71 ± 0.76	0.33 ± 0.06	2.22 ± 0.14	43.26 ± 0.68
25 mm	40.55 ± 0.78	0.00 ± 0.00	0.82 ± 0.18	41.37 ± 0.81
26 mm	38.40 ± 0.73	2.34 ± 0.11	1.32 ± 0.16	42.07 ± 0.64

3.2. Finite Element Result

3.2.1. Stress distributions

Two cardiac cycles were simulated for each valve in three testing conditions. Maximum in-plane stress contours on six different locations on the flow curve have been reported in Figures 2a and 2b. Maximum stress on leaflets of 25 mm Perimount Magna Ease were at the peak of systole on the fixed boundary edges. The maximum amount of stress in reference adult aortic condition, child pulmonary with normal flow, and child pulmonary with the low flow were 3.14, 3.01, and 1.18 MPA, respectively. However, during diastole, the peak stress values for Perimount Magna Ease reached 764, 729, and 417 KPa in adult aortic, and child pulmonary with normal and low flow, respectively.

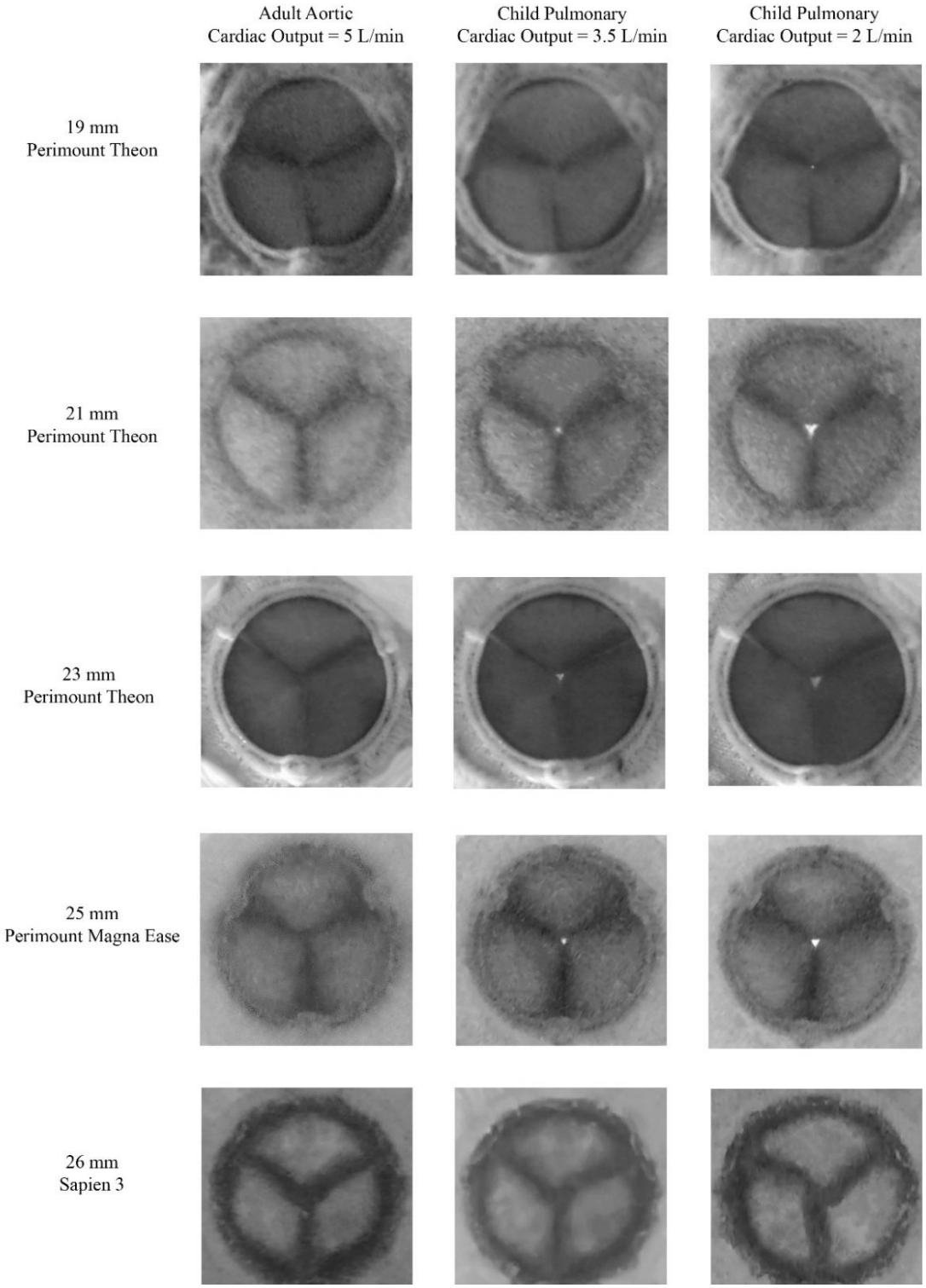

Figure 5.1: Perimount Theon, Perimount Magna Ease, and Sapien 3 valves in closed positions under adult aortic, child pulmonary with normal flow, and child pulmonary with low flow conditions

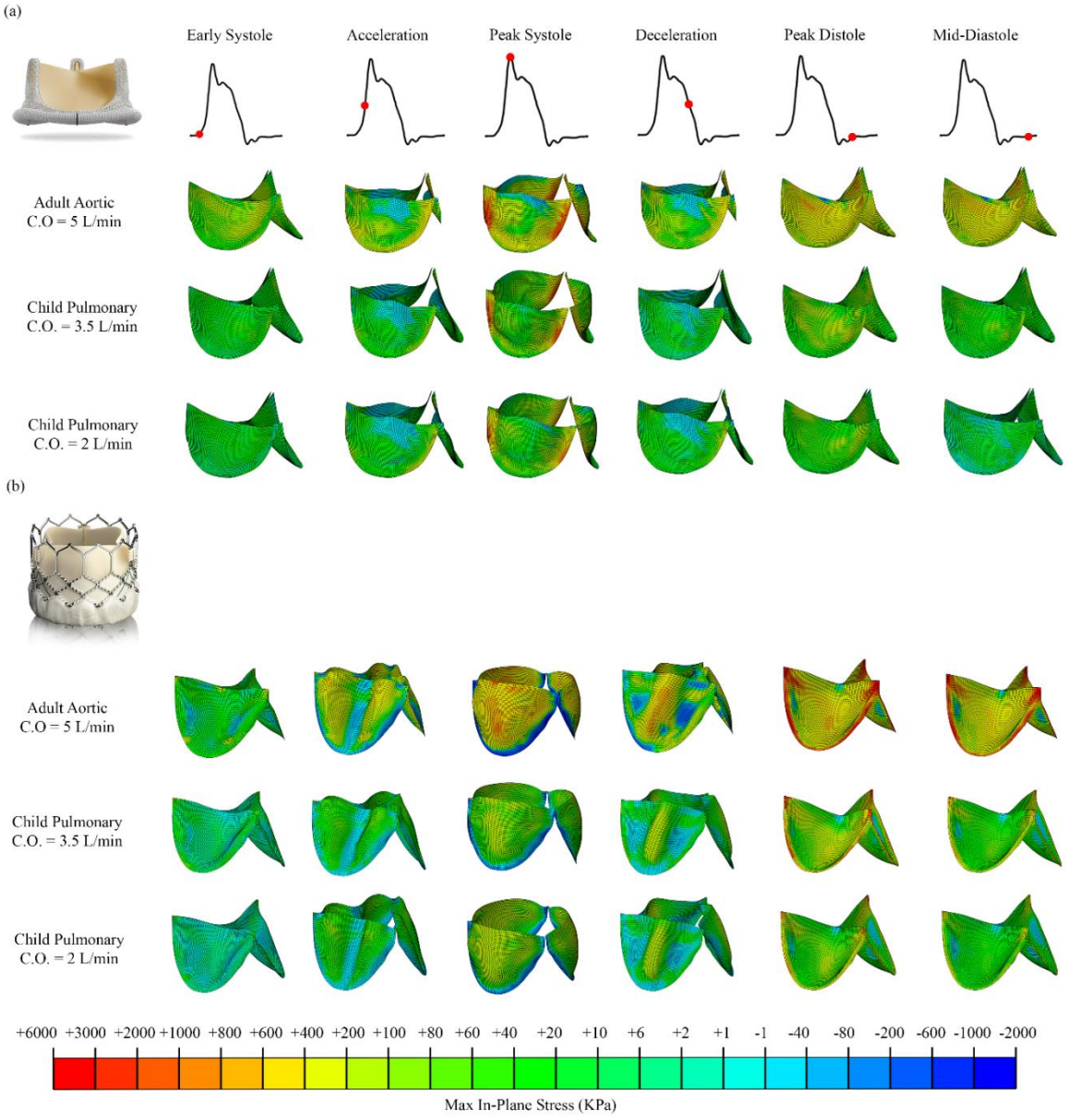

Figure 5.2: Comparison of maximum in-plane stress distribution throughout a complete cardiac cycle for adult aortic and child pulmonary conditions. (a) 25 mm Magna Ease, (b) 26 mm Sapien 3. The maximum stress for Magna Ease is during systole while maximum stress in Sapien 3 is during diastole.

The reported maximum in-plane stress contours for Sapien 3 transcatheter valve show the maximum stress on the leaflets was at the peak of diastole in the fully closed position on the commissural areas. These stress values were 16.7, 9.11, and 2.97 MPA for adult aortic, and child pulmonary with normal and low flow, respectively. While at the peak of systole, the values of maximum stress were recorded as 2.06, 1.48, and 0.21 MPA in adult aortic and child pulmonary with normal and low flow conditions.

Comparing the stress distributions on both valves shows that 25 mm Perimount Magna Ease experienced more stress at the peak of systole. More stress values on transcatheter Sapien 3 valve at the peak of diastole could be because the leaflets have smaller thicknesses than the 25 mm surgical valve.

3.3. Conclusion

In this study, we examined the risks associated with pulmonary valve replacement. The results of experiments showed that the amount of paravalvular regurgitation from the surgical valve is a risk factor after Magna Ease valve implantation after SPVR in pediatric patients. On the other hand, the maximum opening area at the peak of systole indicates that the degree of opening in Sapien 3 valve is less in pulmonary conditions than the aortic condition. Less opening area after TPVR with Sapien 3 valve may increase the risk of blood stasis and initiate subclincal leaflet thrombosis in patients. Leaflet thrombosis is a major complication after TPVR and it increases the possibility of the reintervention.

Long-term durability of the valve inside the patient's body is another important factor that is still under investigations and there is still paucity of clinical data regarding the durability of the vales. We used finite element method as a tool to estimate the occurrence

of structural deterioration of the valves as a result of fatigue in the leaflets. According to finite element simulations, higher stress values in Sapien 3 comparing to the surgical valves in pulmonary conditions could lessen the longevity of the Sapien 3 valve. Because higher stress on the leaflets accelerate the tissue degeneration and reduces the life of the bioprosthetic valves.

Therefore, using Sapien 3 valve in the pulmonary position may seem to be a less invasive solution with promising outcomes for pulmonary insufficiencies, but major complications such as thrombosis and longevity of the valves need to be taken into account.

3.4. Discussion

The present study evaluated the off-label use of 3 commercial aortic bioprostheses (i.e. Edwards Theon, Edwards Magna Ease, and Edwars Sapien 3) under pulmonic conditions for pediatric patients using an in-vitro pulse duplicator setup. The pressure gradient, degree of opening, regurgitation volume, and energy loss for different sizes of surgical and transcatheter bioprosthetic valves were compared. The leaflet motions, captured by a high-speed camera during in-vitro tests, were used for non-invasive leaflet material properties characterization. Moreover, the stress distribution and leaflet deformation in two complete cardiac cycles of 25 mm Magna Ease and 26 mm Sapien 3 valve were assessed in finite element simulations using the optimized material properties.

According to the limitations in size and other complications like stent fracture of commercially available pulmonary bioprosthetic heart valves in the market, the off-label use of aortic bioprosthesis for native RVOTs has increased in past years. However, choosing a durable bioprosthesis for pulmonary valve replacement is the main concern

since available clinical data in the literature mainly include the early and midterm outcomes for patients who have undergone off-label implantation, and there is paucity of data regarding long-term care outcomes. The long-term durability of tissue depends on multiple factors, including mechanical damage and calcification. Therefore, the application of computational simulations to determine high-stress regions on the leaflets and their correlation with calcified prone regions can be utilized to estimate the lifespan of a bioprosthesis and compare the durability of available bioprosthetic heart valve options in the market.

Hallbergson et al. studied late postoperative outcomes of patients who underwent SPVR with bovine pericardium after Tetralogy of Fallot repair. The promising result has been shown in <7 years of follow-ups. However, early right ventricular volumes and regurgitant fraction reduction did not last more than seven years after SPVR, and pulmonary regurgitation gradually increased to 35% of its pre-intervention value. They also showed that the increasing right ventricular volume after SPVR is associated with progressive pulmonary regurgitation, which is related to stenosis.(Hallbergson et al. 2015) Devangondi et al. investigated the long-term incidence of pulmonary regurgitation after TPVR. They showed with the median follow-up of 15.1 years after implantation, about 60% of the patients suffered from moderate or severe pulmonary regurgitation, which led to reintervention in 22% after 20 years. They also concluded that younger age was the critical factor associated with moderate or severe pulmonary regurgitation.(Devanagondi et al. 2017) Moreover, Abbasi et al. have developed a computational model to find stress distribution on different aortic bioprosthetics, including Magna Ease and Sapien 3. The

higher stress regions in Magna Ease and Sapien 3 were found in fixed boundary edges and commissural areas during systole and diastole, respectively. They found out these higher stress regions in Sapien 3 were 35% bigger than areas in Magna Ease which may contribute to the higher tissue degeneration rate of leaflets (Abbasi et al. 2019). However, there are no such investigations on the right side of the heart. Therefore, in the present study, we showed that the long-term durability of transcatheter and surgical aortic boiprostheses in pulmonary position might differ according to the recorded stress values in finite element simulations.

In addition, we conducted a comparison of the mobility of bioprostheses in the pulmonary position. We showed that Sapien 3 valve opening area in pulmonary conditions is less than the aortic condition, which leads to blood stasis, increases the risk, and initiates blood stasis. Our finding is confirmed by the available clinical data in the literature, which shows cases of developed subclinical leaflet thrombosis in short-term follow-ups after TPVR. Hammadah et al. performed a study on the incidence of reduction in the degree of valve opening resulting in subclinical leaflet thrombosis after Sapien 3 valve implantation. They concluded that the under-expansion of the transcatheter valve in both native valves and valve-in-vale procedures contributes to subclinical thrombosis and may result in reduced valve durability and increased risk of reintervention over time.(Hammadah et al. 2021) Riahi et al. reported a case of subclinical leaflet thrombosis within a 30-day follow-up after Sapien 3 implantation in a native RVOT. They determined that, over time, early thrombosis contributes to valve dysfunction. Hascoet et al. reviewed the result of Sapien 3

valve implantation in a short-term follow-up of 14 months for 129 patients and detected no complications other than the development of leaflet thrombosis.(Hascoet et al. 2019)

3.5.Limitations

With the development of new medical devices, such as Medtronic Harmony and Edwards Alterra adaptive present, the transcatheter valve replacement is expanding for the treatment of pulmonary regurgitation in patients with native RVOTs. In this study, we tried to address a few concerns regarding the off-label use of Sapien 3 and show that the performance of aortic bioprosthetics is not equivalent to pulmonary conditions. However, to solidify this study's result, the major limitations must be covered in future works. Some of these limitations are discussed in the following paragraphs.

First, the material optimization was performed using the average distance of the middle point on each leaflet. However, since the accuracy of the simulations is related to the accuracy of the material properties of the leaflets, the simultaneous displacement of all three leaflets must be considered for the optimization framework. Second, the stress distribution results came from the analysis of only one valve size, while there are always some variations in leaflet thicknesses and material properties. Therefore, repeating the same procedure on several valves and further statistical analysis are required to generalize this study's findings. We also used a damping coefficient in the simulations to mimic the viscous damping effects of the blood. More complex simulations, like fluid-solid interaction, may be required to evaluate the amount of shear stress applied to the leaflets. Additionally, the result of finite element simulations must be validated by more comprehensive experiments. Finally, the exact geometry of the valves is required for

simulations since the geometry we developed is only close to the actual valve and is not precisely the same.

Bibliography

Abbasi, Mostafa, Mohammed S Barakat, Danny Dvir, and Ali N Azadani. 2019. "A non-invasive material characterization framework for bioprosthetic heart valves." *Annals of biomedical engineering* 47 (1):97-112.

Apitz, Christian, Gary D Webb, and Andrew N Redington. 2009. "Tetralogy of fallot." *The Lancet* 374 (9699):1462-1471.

Association, Glycerine Producers'. 1963. *Physical properties of glycerine and its solutions*: Glycerine Producers' Association.

Balzer, David. 2019. "Pulmonary valve replacement for tetralogy of Fallot." *Methodist DeBakey cardiovascular journal* 15 (2):122.

Barakat, Mohammed, Danny Dvir, and Ali N Azadani. 2018. "Fluid dynamic characterization of transcatheter aortic valves using particle image velocimetry." *Artificial Organs* 42 (11):E357-E368.

Benson, Lee N, Matthew J Gillespie, Lisa Bergersen, Sharon L Cheatham, Kan N Hor, Eric M Horlick, Shicheng Weng, Brian T McHenry, Mark D Osten, and Andrew J Powell. 2020. "Three-year outcomes from the harmony native outflow tract early feasibility study." *Circulation: Cardiovascular Interventions* 13 (1):e008320.

Bergersen, Lisa, Lee N Benson, Matthew J Gillespie, Sharon L Cheatham, Andrew M Crean, Kan N Hor, Eric M Horlick, Te-Hsin Lung, Brian T McHenry, and Mark D Osten. 2017. "Harmony feasibility trial: acute and short-term outcomes with a self-expanding transcatheter pulmonary valve." *JACC: Cardiovascular Interventions* 10 (17):1763-1773.

Bonhoeffer, Philipp, Younes Boudjemline, Shakeel A Qureshi, Jerome Le Bidois, Laurence Iserin, Philippe Acar, Jacques Merckx, Jean Kachaner, and Daniel Sidi. 2002. "Percutaneous insertion of the pulmonary valve." *Journal of the American College of Cardiology* 39 (10):1664-1669.

Bonhoeffer, Philipp, Younes Boudjemline, Zakhia Saliba, Ana Olga Hausse, Yacine Aggoun, Damien Bonnet, Daniel Sidi, and Jean Kachaner. 2000. "Transcatheter implantation of a bovine valve in pulmonary position: a lamb study." *Circulation* 102 (7):813-816.

Butera, Gianfranco, Ornella Milanesi, Isabella Spadoni, Luciane Piazza, Andrea Donti, Christian Ricci, Gabriella Agnoletti, Alberta Pangrazi, Massimo Chessa, and Mario Carminati. 2013. "Melody transcatheter pulmonary valve implantation. Results from the registry of the Italian Society of Pediatric Cardiology." *Catheterization and Cardiovascular Interventions* 81 (2):310-316.

Chandran, Krishnan B, Stanley E Rittgers, and Ajit P Yoganathan. 2006. *Biofluid mechanics: the human circulation*: CRC press.

Daily, Joshua A, Xinyu Tang, Michael Angtuaco, Elijah Bolin, Sean M Lang, and R Thomas Collins II. 2018. "Transcatheter versus surgical pulmonary valve replacement in repaired tetralogy of Fallot." *The American Journal of Cardiology* 122 (3):498-504.

Devanagondi, Rajiv, Dan Peck, Janaki Sagi, Janet Donohue, Sunkyung Yu, Sara K Pasquali, and Aimee K Armstrong. 2017. "Long-term outcomes of balloon valvuloplasty for isolated pulmonary valve stenosis." *Pediatric cardiology* 38 (2):247-254.

DeZorzi, Christopher J, Justin P Sheehy, Adnan Chhatriwalla, Anthony Magalski, and John T Saxon. 2021. "Intracardiac Echocardiography to Diagnose Bioprosthetic Pulmonary Valve Thrombosis." *Case Reports* 3 (4):682-685.

Fathallah, Mouhammad, and Richard A Krasuski. 2017. "Pulmonic valve disease: review of pathology and current treatment options." *Current cardiology reports* 19 (11):1-13.

Ghawi, Hani, Damien Kenny, and Ziyad M Hijazi. 2012. "Transcatheter pulmonary valve replacement." *Cardiology and Therapy* 1 (1):1-14.

Hallbergson, Anna, Kimberlee Gauvreau, Andrew J Powell, and Tal Geva. 2015. "Right ventricular remodeling after pulmonary valve replacement: early gains, late losses." *The Annals of thoracic surgery* 99 (2):660-666.

Hammadah, Muhammad, B Kelly Han, Mariana de Oliveira Nunes, Jamil A Aboulhosn, Evan M Zahn, Vasilis Babaliaros, Matthew J Daniels, João L Cavalcante, John R Lesser, and Santiago Garcia. 2021. "Hypoattenuated Leaflet Thickening After Transcatheter Pulmonary Valve Replacement With the SAPIEN 3 Valve." *Cardiovascular Imaging*.

Hascoet, Sebastien, Robert Dalla Pozza, Jamie Bentham, Ronald Giacomo Carere, Majed Kanaan, Peter Ewert, Elzbieta Katarzyna Biernacka, Oliver Kretschmar, Cornelia Deutsch, and Florence Lecerf. 2019. "Early outcomes of percutaneous pulmonary valve implantation using the Edwards SAPIEN 3 transcatheter heart valve system." *EuroIntervention* 14 (13):1378-1385.

Head, Stuart J, Mevlüt Çelik, and A Pieter Kappetein. 2017. "Mechanical versus bioprosthetic aortic valve replacement." *European heart journal* 38 (28):2183-2191.

Jang, WooSung, Yong Jin Kim, Kwangho Choi, Hong-Gook Lim, Woong-Han Kim, and Jeong Ryul Lee. 2012. "Mid-term results of bioprosthetic pulmonary valve replacement in pulmonary regurgitation after tetralogy of Fallot repair." *European Journal of Cardio-Thoracic Surgery* 42 (1):e1-e8.

Kenny, Damien, John F Rhodes, Gregory A Fleming, Saibal Kar, Evan M Zahn, Julie Vincent, Girish S Shirali, Jeremy Gorelick, Mark A Fogel, and John T Fahey. 2018. "3-year outcomes of the Edwards SAPIEN transcatheter heart valve for conduit failure in the pulmonary position from the COMPASSION multicenter clinical trial." *JACC: Cardiovascular Interventions* 11 (19):1920-1929.

Kheradvar, Arash, Elliott M Groves, Craig J Goergen, S Hamed Alavi, Robert Tranquillo, Craig A Simmons, Lakshmi P Dasi, K Jane Grande-Allen, Mohammad RK Mofrad, and Ahmad Falahatpisheh. 2015. "Emerging trends in heart valve engineering: Part II. Novel and standard technologies for aortic valve replacement." *Annals of biomedical engineering* 43 (4):844-857.

Morgan, Gareth, Pimpak Prachasilchai, Worakan Promphan, Eric Rosenthal, Kothandam Sivakumar, Mahesh Kappanayil, Indriwanto Sakidjan, Kevin P Walsh, Damien Kenny, and John Thomson. 2019. "Medium-term results of percutaneous pulmonary valve implantation using the Venus P-valve: international experience." *EuroIntervention* 14 (13):1363-1370.

Nomoto, Rio, Lynn A Sleeper, Michele J Borisuk, Lisa Bergerson, Frank A Pigula, Sitaram Emani, Francis Fynn-Thompson, John E Mayer, J Pedro, and Christopher W Baird. 2016. "Outcome and performance of bioprosthetic pulmonary valve replacement in patients with

congenital heart disease." *The Journal of thoracic and cardiovascular surgery* 152 (5):1333-1342. e3.

Nordmeyer, Johannes, Philipp Lurz, Victor T Tsang, Louise Coats, Fiona Walker, Andrew M Taylor, Sachin Khambadkone, Marc R de Leval, and Philipp Bonhoeffer. 2009. "Effective transcatheter valve implantation after pulmonary homograft failure: a new perspective on the Ross operation." *The Journal of Thoracic and Cardiovascular Surgery* 138 (1):84-88.

Pragt, Hanna, Joost P van Melle, Gijsbertus J Verkerke, Massimo A Mariani, and Tjark Ebels. 2020. "Pulmonary versus aortic pressure behavior of a bovine pericardial valve." *The Journal of thoracic and cardiovascular surgery* 159 (3):1051-1059. e1.

Rao, P Syamasundar. 2007. "Percutaneous balloon pulmonary valvuloplasty: state of the art." *Catheterization and Cardiovascular Interventions* 69 (5):747-763.

Rosseel, Liesbeth, Ole De Backer, and Lars Søndergaard. 2019. "Clinical valve thrombosis and subclinical leaflet thrombosis following transcatheter aortic valve replacement: is there a need for a patient-tailored antithrombotic therapy?" *Frontiers in cardiovascular medicine* 6:44.

Schneider, Andrew E, Jeffrey W Delaney, and Allison K Cabalka. 2016. "Non-infectious thrombosis of the melody® valve: A tale of two cities." *Catheterization and Cardiovascular Interventions* 88 (4):600-604.

Shahanavaz, Shabana, Evan M Zahn, Daniel S Levi, Jamil A Aboulhousn, Sebastien Hascoet, Athar M Qureshi, Diego Porras, Gareth J Morgan, Holly Bauser Heaton, and

Mary Hunt Martin. 2020. "Transcatheter pulmonary valve replacement with the Sapien prosthesis." *Journal of the American College of Cardiology* 76 (24):2847-2858.

Shinkawa, Takeshi, Chiajung K Lu, Carl Chipman, Xinyu Tang, Jeffrey M Gossett, and Michiaki Imamura. 2015. "The midterm outcomes of bioprosthetic pulmonary valve replacement in children." Seminars in thoracic and cardiovascular surgery.

Spigel, Zachary A, Iki Adachi, Ziyad M Binsalamah, Dhaval Parekh, and Athar M Qureshi. 2021. "Transcatheter pulmonic valve implantation in adult patients with prior congenital heart surgery." *Annals of cardiothoracic surgery* 10 (5):658.

Tan, Weiyi, Ada C Stefanescu Schmidt, Eric Horlick, and Jamil Aboulhosn. 2022. "Transcatheter Interventions in Patients With Adult Congenital Heart Disease." *Journal of the Society for Cardiovascular Angiography & Interventions*:100438.

Zahn, Evan M, Jennifer C Chang, Dustin Armer, and Ruchira Garg. 2018. "First human implant of the Alterra Adaptive PrestentTM: A new self-expanding device designed to remodel the right ventricular outflow tract." *Catheterization and Cardiovascular Interventions* 91 (6):1125-1129.